Accepted manuscript doi: 10.1680/jener.19.00055

Accepted manuscript doi: 10.1680/jener.19.00055

Submitted: 13 June 2019

Published online in 'accepted manuscript' format: 01 October 2020

Manuscript title: Performance and emissions of spark-ignition engines fuelled with petrol and methane

Authors: Yasin Karagöz[1], Özgün Balcı[2], Onur Gezer[2], Hasan Köten[1] and Övün Işın[2]

Affiliations: [1]Department of Mechanical Engineering, Engineering Faculty, Istanbul Medeniyet University, Kadıköy, Istanbul, 34000, Turkey and [2]Automotive Division, Department of Mechanical Engineering, Mechanical Engineering Faculty, Yildiz Technical University, Yildiz, Besiktas, Istanbul, 34349, Turkey

Corresponding author: Yasin Karagöz, Department of Mechanical Engineering, Engineering Faculty, Istanbul Medeniyet University, Kadıköy, Istanbul, 34000, Turkey.

E-mail: yasin.karagoz@medeniyet.edu.tr

Accepted manuscript doi:
10.1680/jener.19.00055

Abstract

Diesel engines using compression ignition are increasingly prohibited in cities because of increased environmental concerns. This could lead to greater use of low-powered spark-ignition engines in hybrid electrical cars. Using alternative fuels is important for spark-ignition engines. In the study reported in this paper, performance and in-cylinder pressure data were collected from petrol- and methane-fuelled spark-ignition engines. A theoretical engine model was then verified using experimental data. The theoretical results for methane and petrol were finally compared for different engine speeds. The theoretical model used a combustion model and chemical kinetics model to compare the effects of methane and petrol on engine performance and emissions at different engine speeds. Thanks to the high knock resistance of methane, the most suitable ignition advance value was decided for the methane-fuelled simulation by considering the maximum thermal efficiency to limit assumed reductions in indicated thermal efficiency and indicated mean effective pressure compared to previous studies. A slight reduction in nitrous oxides and carbon monoxide emissions was observed when using methane at full load.

Keywords: pollutant; pollution; spark ignition engine; alternative gaseous fuel; combustion simulation; ignition advance; energy conservation; environment

Accepted manuscript doi: 10.1680/jener.19.00055

1. Introduction

In recent years, not only has the number of diesel vehicles increased but also the rate of growth has increased in vehicle park (EEA, 2017). This situation causes environmental concerns, especially due to nitrous oxides and particulate matter (EEA, 2016a). To mitigate the problem, the use of diesel vehicles in urban centres have been restricted at differentvarious locations around the world (EPCA, 2017; Transport for London, 2016).

In recent years, research and development studies have been accelerated on electric-motor-powered vehicles, but there are still issues such as insufficient battery storage capacity, limited availability of charging stations and excessive charging times in this scenario. Adequate improvements about mentioned electric vehicle problems requires time (EEA, 2016b). On the other hand, the reduction in fossil fuel reserves, in parallel with the world's increasing energy demand, is also a serious problem. For this reason, switching to biofuels instead of conventional fuels in road transport has substantial importance in terms of both energy supply and emission control (Costagliola et al., 2016; Iodice, Langella and Amoresano 2018; Iodice and Senatore, 2016).

Therefore, power-pack systems with low-power spark-ignition (SI) engines operated with alternative fuels are predicted to become widespread. Using these alternative gas-powered power units, which can be used in serial or parallel with electric motors in hybrid vehicles, provides a great advantage, especially in urban traffic conditions.

Methane is an environmental-friendly fuel for internal combustion engines with low carbon/hydrogen ratio and wide flammability limits (Pan et al., 2018). Additionally, it is known that methane is a gaseous fuel and this situation enhances the homogeneity of the air-fuel mixture. Also, methane has benefits in terms of emissions thanks to high hydrogen content (Pan et al., 2018). Some further physicochemical properties of petrol and methane fuels can be found in Table 1. Natural gas contains methane in high proportion and methane is one of the major component of natural gas and methane does not contain carbon-to-carbon chemical bonds (Lyu et al., 2017). The use of methane in SI engines is a realistic approach today, since natural gas is more economic fuel than diesel fuel (Hu et al., 2017). The studies which using methane and natural gas in SI engines are summa*rise*d in the next paragraph.

Irimescu, Vasiu and Tordai (2014) investigated the performance parameters of methane and petrol in SI engine experimentally. This study shows that if the ignition advance is optimized when using the methane as an energy source, the combustion efficiency increases compared to petrol. Both fuel types have similar characteristics in terms of heat losses. Gharehghani *et al.* (2015) used a four-cylinder naturally aspirated engine in their experimental study and they compared CNG (compressed natural gas) and petrol. According to results which obtained from this study, the engine power output increases, but thermal efficiency slightly decreases when petrol was used as fuel. Higher exergy efficiency has been achieved with the use of CNG. Tahir *et al.* (2015) observed in their study that the use of CNG causes lower in-cylinder pressure values and lower power output than petrol. The authors claimed that the volumetric efficiency decreases when using CNG. In case of using CNG in-cylinder pressure reduction up to 20%, heat losses reduction up to 23% and output power reduction up to 18.5% were observed compared to that of petrol.

In some studies, natural gas was used in liquid form, which known as LNG. Chen *et al.* (2017) were interested in methane content of LNG fuel in their experimental study. Two different fuel composition were used in this study which included 93% and 99% methane proportionally. The study have been carried out with three different compression ratio and ignition advance values. According to results, the blend which includes 99% methane has the highest knock resistance. At full load condition, the BSFC had lowest value with using 99%

methane fuel, because methane has higher knock resistance and ignition timing can be advanced.

In some studies carried out, which are mentioned in this paragraph, the hydrogen and methane blends were used in SI engines. Moreno *et al.* (2012) examined the effect of fuel content by blending hydrogen and methane at different rates for naturally aspirated SI engine. The hydrogen concentration in the fuel blend was increased up to 50% volumetrically. It was observed that as the methane ratio decreased, NO_x emissions and BTE decreased. Akansu, Kahraman and Çeper (2007) used a four cylinder engine in their experimental study and they blended hydrogen and methane in different ratios volumetrically. The studies conducted under 2000 rpm engine speed and constant engine load. They obtained that BTE and NO increased, HC and carbon monoxide and carbon dioxide decreased as the hydrogen concentration increased.

In some studies, methane was used as a fuel blend with some hydrocarbons such as propane, butane etc. for SI engines. Montoya, Amell and Olsen (2016) used a four stroke, single cylinder SI engine, of which compression ratio can adjust between 4 and 18, and they used methane-hydrogen and propane-hydrogen blends as fuel. From this study, it has been seen that, methane-hydrogen blends have higher knock resistance and higher thermal efficiency than propane-hydrogen blends. Amirente *et al.* (2017) used a single-cylinder, port injection, spark ignition engine in their study. They used pure methane, pure propane, propane-methane mixture and natural gas under stoichiometric air-fuel ratio and full load condition at 2000 rpm, 3000 rpm, 4000 rpm engine speeds. The ratio of methane in the methane-propane mixture varied between 10% and 40%. It is evident from results of their work, changes in the rate of propane and methane has significant effect on performance and emission parameters. While propane ratio increases, the complete combustion improves, indicated mean effective pressure (IMEP) and NO_x increase due to higher in-cylinder temperatures.

In some studies, which are mentioned in this paragraph, the biogas fuel has been used in SI engines. Subramanian *et al.* (2013) compared methane enriched biogas (93% methane) and base CNG (89.14% methane) fuel in SI engine for the Indian driving Cycle (MIDC). In terms of fuel economy, there is no significant difference between enriched biogas and base CNG fuel. Also, no visible difference was observed in carbon dioxide emissions per kilometre. Using methane enriched biogas fuel in SI engine, decreases carbon monoxide, hydrocarbon (HC) and nitrous oxides (NO_x) emissions slightly.

Even though many studies about methane were carried out in the literature, none of the studies have used a single cylinder, extremely light duty engine which can be used in a small power-pack as range extender for hybrid systems in the near future. Although there are many studies about different alternative gaseous fuel mixtures in the literature, in this study the use of pure methane fuel was investigated, because using natural gas in SI engines is a feasible, realistic and economical method. It has also been emphasized that small power (old technology carburetted) engines can be calibrated and converted into methane fuel, taking into account of the maximum ITE map and appropriate ignition advance, by means of an attached injection system, quickly and experimentally verified by a numerical model. On the other hand, firstly the experimental studies with petrol and methane fuels were completed, then mathematical model was verified. Also, the optimum ignition advance was determined considering maximum indicated thermal efficiency values for methane fuel. Lastly, acquired combustion characteristics (in-cylinder pressure, heat release rate), emission and performance values were compared with neat petrol and methane fuels.

2. Material and methods

Figure 1 shows a schematic view of the engine test setup in the laboratory. Schematic figure shows that test bench consists of SI engine loaded by dynamometer and external resistive load banks, sensors which were installed to collect intake air flow, in-cylinder pressure, crank position, engine speed, fuel consumption and emission data and post processing system.

Experimental process was conducted at 2650 rpm and 3400 rpm engine speeds. Both, experimental setup and theoretical models are built according to run at stoichiometric conditions for petrol and methane fuels. Stoichiometric air-fuel ratios of the petrol and methane were assumed as 14.6 and 17.24, respectively.

2.1. Experimental setup

A single-cylinder, four-stroke, 270 cm^3, air-cooled, naturally aspirated spark-ignition engine was used in experiments. The engine was loaded by an alternative current dynamometer.

The sensor group includes a mass flowmeter to measure intake air mass flow rate, a spark plug type Kistler 6118B in-cylinder pressure transducer, an incremental type encoder to evaluate crank position and engine speed data, a miniature oval gear type fuel flow meter to determine the fuel consumption and AVL Digas 4000 gas analyser to measure exhaust gases emissions.

In the experimental tests, the data which were collected from in-cylinder pressure sensor, were sent to Kistler Ki-Box combustion analyser device and recorded for post processing.

Accepted manuscript doi: 10.1680/jener.19.00055

For the determination of specific exhaust gases emissions, mass flow rate of intake air data and emission data were used and the method that specified in VDMA exhaust emission legislation for gas engines, was used in calculations.

2.2. Engine specifications and dynamometer features

In this experimental study, natural aspirated, ai- cooled, four-stroke, single-cylinder, spark-ignition, Honda engine which has 270 cm^3 engine swept volume was used. Further information about the engine and dynamometer is given in Table 2.

2.3. SI engine model

A 270 cm^3, single-cylinder SI engine used in the engine tests was mathematically modelled with the help of AVL Boost software, which reaches the result with both one-dimensional (quasi-dimensional) model and zero-dimensional model. Intake and exhaust lines are determined as one-dimensionally by using the finite element method, and in-cylinder behaviours are determined according to zero-dimensional thermodynamic approaches. The friction model in the programme was run to obtain FMEP depending on the speed and indicated pressure. Piston and bore diameter, stroke, compression ratio, connecting rod length and the clearance distance that may lead to blow-by leakage are entered to determine combustion chamber geometry and local loss coefficients were entered in the programme.

The parameters of the engine model and Vibe 2 Zone combustion model, which was used in this study, were determined by using experimentally obtained data. Two zone vibe is a model that preferred in many academic studies. In two zone vibe modelling, the combustion chamber is divided in two regions where one of the flame has not yet reached and the other

Accepted manuscript doi: 10.1680/jener.19.00055

region composed of combusted area. AVL Boost software contains a sub-programme BURN which determines the heat release rate values considering the heat transfer (Rimkus et al., 2015). K-epsilon model was chosen as the turbulence model. The K-epsilon model gives very good results in determining both the regions where the flame has not yet reached and the flame propagation regions movements (Sjerić et al., 2016). This also reveals the co-operation compatibility with the two-zone vibe combustion model. Laminar flame velocity was modelled in accordance with Metghalchi and Keck correlation, and turbulence burning velocity was modelled in accordance with Bradley correlation, as in the study (Gupta and Abdel-Gayed, 2015). The heat transfer model is built by using Woschni, which is highly preferred in the literature and instantly solves heat transfer.

Petrol and methane fuels were chosen for simulations from Classic Species Setup of AVL Boost software which used by programme to calculate combustion kinetics and intermediary reactions, and hence emissions. Figure 2 depicts the schematic view of the theoretical model of the test engine. The Vibe model in the study was used in order to get fast results and to be a methodology in which methane calibration can be performed quickly.

3. Data reduction

Indicated mean effective pressure can be calculated as shown in Equation (3) (Heywood, 1988) by using indicated engine work as given in Equation (2) (Heywood, 1988).

$$V = \frac{V_H}{2}\left[(1 - cos\,\alpha\,) + \frac{\lambda}{4}(1 - cos2\alpha)\right] + \frac{V_H}{\varepsilon - 1} \quad (1)$$

$$W_i = \int_0^{720} P\, dV \quad (2)$$

$$P_{mi} = \frac{W_i}{V_H} \quad (3)$$

Accepted manuscript doi:
10.1680/jener.19.00055

where, V is instant cylinder volume (m^3) calculated in Equation (1), V_H is cylinder displacement (m^3), λ is ratio of crank radius to connecting rod length, α is crank angle (degree), ε is compression ratio of the engine, W_i is indicated work of the engine per cycle (J), P_{mi} is mean indicated pressure (Pa) and P is measured in-cylinder pressure (Pa).

Indicated thermal efficiency can be calculated as seen in Equation (5) (Bauer and Forest, 2001) by using indicated torque value which was stated in Equation (4).

$$N_i = \frac{W_i \; x \; n}{60 \; x \; 2} \tag{4}$$

$$ITE = \frac{N_i}{\dot{m}_f \times LHV_f} \tag{5}$$

where, N_i is indicated engine power (kW), n is engine speed (rpm), ITE is indicated thermal efficiency, $\dot{m}_f$ is mass flow rates of fuels (petrol or methane) (kg/s) and LHV_f is lower heating values of fuels (petrol or methane) (kJ/kg).

Heat release rate calculations from the experimental data were realized as shown in Equation (6) (Egnell, 1998).

$$\dot{Q} = \frac{k}{k-1} P \frac{dV}{d\theta} + \frac{k}{k-1} V \frac{dP}{d\theta} \tag{6}$$

where, $\dot{Q}$ is heat release rate (HRR) (J/^{o}CA) and k is working mixture polytrophic index.

On the other hand, Vibe 2 Zone approximation, which was used as combustion model of theoretical engine model in this study, calculates heat release rate values by using vibe function as shown in Equation (7), (8) and (9) (AVL, 2013).

$$\frac{dx}{d\alpha} = \frac{\alpha}{\Delta\alpha_c}(m+1) y^m e^{-\alpha \, y^{(m+1)}} \tag{7}$$

$$dx = \frac{dQ}{Q} \tag{8}$$

$$y = \frac{\alpha - \alpha_0}{\Delta\alpha_c} \tag{9}$$

where, Q is total fuel heat input, α is crank angle, α_0 is crank angle at the beginning of combustion, $\Delta\alpha_c$ is combustion duration, m is shape parameter, a is Vibe parameter which is equal to 6.9 for complete combustion. The parameters of Vibe function are approximated by also using mass fraction burned Equation of Vibe.

Exhaust emissions were measured using gas analyser by volume while executing the tests. Mass flow rate of total exhaust gases can be calculated by adding measured flow rate of intake air and consumed fuel as seen in Equation (10) (VDMA, 2017). Consequently, specific emissions can be obtained as shown in Equation (11) (VDMA, 2017).

$$\dot{m}_{exh} = \dot{m}_{int} + \dot{m}_f \qquad (10)$$

$$EP_i = EV_i \; x \; \frac{M_i}{M_{exh}} \; x \; \frac{\dot{m}_{exh}}{N_i} \qquad (11)$$

where, $\dot{m}_{exh}$ and $\dot{m}_{int}$ is mass flow rates of exhaust gases and intake air, respectively (g/h), EP_i is specific emission value of relevant gases (g/kWh), EV_i is relevant gases amount in proportion to total exhaust gases (by volume for carbon monoxide and by particle count for THC and NO_x) and M_i and M_{exh} are molar mass of relevant gases and exhaust gases respectively (kg/kmol).

Kline and Mc Clintock analysis (Kline and McClintock, 1953) determined the total propagated uncertainty of the Precision and Systematic (Bias) errors measurement as:

$$(W_R)_{P,B} = \left[\left(\frac{\partial R}{\partial x_1} w_1\right)^2 + \left(\frac{\partial R}{\partial x_2} w_2\right)^2 + \cdots + \left(\frac{\partial R}{\partial x_n} w_n\right)^2\right]^{1/2} \qquad (12)$$

Hence, the total uncertainty W_R is computed with:

$$W_R = \sqrt{(W_R)_P{}^2 + (W_R)_B{}^2} \qquad (13)$$

where, $(W_R)_{P,B}$ denotes the propagated uncertainty for either precision error $(W_R)_P$, or systematic (Bias) error $(W_R)_B$ functions. $x_1, x_2, \ldots, x_n$ are the measured variables and $w_1, w_2, \ldots w_n$ are the corresponding uncertainties of the variables.

4. Test procedure

In the experimental part of this study, 270 cm^3 SI engine was run at 2650 rpm and 3400 rpm engine speeds at full load condition. All tests were run at stoichiometric air-fuel ratio. In-cylinder pressure data, fuel consumption and emissions were measured and collected at these working conditions. In the experiments, a spark plug-type pressure sensor was located in the middle of the combustion chamber due to constructive restrictions. Hence, collected pressure data was highly exposed to pressure fluctuation in the combustion chamber. In order to avoid fluctuant data, embedded filter was used in Kistler combustion analyser device. Then, the theoretical model for spark ignition engines was created by using collected data and determined combustion model parameters.

4.1. Petrol-fuelled validation

For validation of the mathematical model with petrol, in-cylinder pressure and heat release rate data which were acquired from experimental study, were compared and examined at 2650 rpm and 3400 rpm engine speed.

Figure 3 and Figure 4 show the variations of in-cylinder pressure and normalized heat release rate values which were obtained from experimental results and mathematically modelled studies with petrol at 2650 rpm. Figure 5 and Figure 6 show also these values at 3400 rpm engine speed. The maximum in-cylinder pressure values were obtained as 36.11 bar for experimental method and 35.17 bar for simulation results, respectively. The maximum normalized heat release rate values at 2650 rpm engine speed were 0.0358 $1/^{o}CA$ and 0.0329 $1/^{o}CA$. At 2650 rpm and 3400 rpm engine speeds, errors between experimental data and theoretical data were 2.6% and 8.1% (according to experimental data) in terms of maximum in-cylinder pressure and normalized heat release rate, respectively. At 3400 rpm engine speed, maximum in-cylinder pressure values were obtained from the experiments and simulations were 28.35 bar and 27.46 bar, normalized heat release rate values were 0.0246 $1/^{o}CA$ and 0.0267 $1/^{o}CA$, and percentage errors were 3.1% and 8.5%, respectively.

As mentioned before, in-cylinder pressure data were obtained by using a spark-plug type pressure transducer, which was located in the middle of combustion chamber, hence highly exposed to pressure fluctuations. On the other hand, Kibox combustion analyser device has its own filtering process during pressure data acquisition. However, derivative of pressure term in Equation (6) causes additional fluctuations in HRR variations, in spite of filtered pressure data (Yu et al., 2020; İlhak et al., 2020; Geo et al., 2019; Deng et al., 2013).

Above mentioned slightly rough HRR variations, which are seen in Figure 4 and Figure 6, were not filtered in order to conserve original characteristics of the heat release variations.

Variations, which are shown in Figure 3, 4, 5 and 6, has good agreements in terms of their fundamental features, such as the beginning and the end of heat release rate, maximum in-cylinder pressure, maximum heat release rate and in general terms. Therefore, it is concluded that above mentioned results adequately satisfy the validation of theoretical model.

4.2. Methane-fuelled validation

For validation of the mathematical model with methane fuel, in-cylinder pressure data which were acquired from experimental study, were compared and examined at 3400 rpm engine speed.

Accepted manuscript doi:
10.1680/jener.19.00055

Figure 7 shows the variations of in-cylinder pressure which were obtained from experimental results and mathematically modelled studies with using methane at 3400 rpm. The maximum in-cylinder pressure values were obtained as 27.35 bar for experimental method and 26.52 bar for simulation results, respectively. Error between experimental data and theoretically obtained data were 3.0% (according to experimental data) in terms of maximum in-cylinder pressure.

In Figures 3, 5 and 7, the proportional difference between the theoretical and experimental in-cylinder pressure values is high at the beginning of compression. Although the pressure data received through the cylinder has very low values during intake and the beginning of the compression strokes, the pressure sensor, which was used in the tests, is designed for high pressure measurements. Therefore, in mentioned regions, the error ratio is relatively large in proportion to the pressure values obtained from the simulations. This difference is predicted not to cause a fault in the examination of the engine performance, emissions and combustion processes, since it occurs at the intake stroke.

As seen from graphs (Figure 3, 4, 5, 6 and 7), the pressure and heat release rate data of the experimental results and theoretical model results are overlapped. Additionally, other performance and emission values of experimental results and theoretical model results are given in Table 3 and 4. The maximum error ratio was occurred at THC emission with 8.32% for 3400 rpm engine speed with petrol. Consequently, it is seen that these compared values are close enough to confirm the theoretical model.

Experiments were executed in Yildiz Technical University, Internal Combustion Engines Laboratory. The test equipment measurement uncertainties are shown in Table 5.

4.3. Simulations

After the validation, engine performance and emission values were obtained from simulation results for petrol at 2650, 2900, 3150, 3400 and 3650 rpm engine speeds. Then simulations were run for methane fuel at the same engine speeds and engine performance parameter values and emission characteristics were compared for two different fuels at stoichiometric working condition.

Since methane has relatively lower flame speed and higher knock resistance than petrol, simulations were run with higher ignition advance for methane in order to provide maximum indicated thermal efficiency.

5. Results and discussion

In the first step, performance and emission values of the SI engine were obtained experimentally, then the theoretical model was validated by the experimental results. Afterwards, all the results both petrol and methane fuels were obtained theoretically. Also, the results of petrol and methane fuels were compared and examined in terms of in-cylinder pressure, normalized heat release rate, indicated thermal efficiency, indicated mean effective pressure and indicated specific carbon monoxide emission, indicated specific THC emission, indicated specific NO_x emissions.

5.1. Pressure and heat release rate variations

Figure 8 shows in-cylinder pressure variations for petrol and methane fuels at each engine speed. As a result of data which were obtained from theoretical model, the maximum pressure values with using methane fuel at 2650, 2900, 3150, 3400 and 3650 rpm engine speeds drop from 35.17 bar to 32.07 bar, from 32.70 bar to 30.22 bar, from 30.00 bar to 28.58 bar, from 27.46 bar to 26.52 bar, from 25.62 bar to 24.75 bar, respectively.

In methane fuel simulations, the decrease in in-cylinder pressure was limited with using higher ignition advance by the help of high knock resistance of methane. On the other hand, while working with methane fuel, reductions in maximum pressure values can be explained that lower heating value of methane on volume basis and volumetrically energy content in the cylinder are lower than that of gasoline fuel (Thurnheer, Soltic and Eggenschwiler, 2009).

For petrol and methane fuels, the normalized heat release rate variations were compared as seen in Figure 9 for five different engine speed values. Similarly, with using methane fuel rather petrol, the maximum normalized heat release rate values were decreased from 0.0329 1/^{o}CA to 0.0298 1/^{o}CA, from 0.0291 1/^{o}CA to 0.0280 1/^{o}CA, from 0.0270 1/^{o}CA to 0.0260 1/^{o}CA, from 0.0267 1/^{o}CA to 0.0243 1/^{o}CA and from 0.0234 1/^{o}CA to 0.0230 1/^{o}CA, respectively.

The highest decrease in in-cylinder maximum pressure value was detected as 8.8% and the highest decrease in normalized heat releases rate was detected as 9.4% for using methane compared to petrol.

The maximum normalized heat release rate values were decreased with using methane fuel. Because methane has relatively lower burning velocity than petrol. Also, combustion occurs more slowly than petrol, and hence combustion duration is higher than petrol combustion duration.

5.2. Indicated thermal efficiency

Figure 10 shows comparison of indicated thermal efficiency values for petrol and methane at five different engine speeds. The ITE values obtained at the mentioned engine speeds (2650, 2900, 3150, 3400 and 3650 rpm) were observed as 25.04%-22.01%, 25.07%-22.32%, 23.82%-21.53%, 21.69%-19.68%, 20.11%-18.06% for petrol and methane fuels, respectively.

The reduction in thermal efficiency with using methane causes from low flame velocity. Since the combustion duration of methane is longer than gasoline fuel (Di Iorio, Sementa and Vaglieco, 2016; Irimescu, 2013), the petrol combustion process occurs closer to ideal constant volume cycle. Thanks to high knock resistance of methane, ignition timing advanced slightly to limit thermal efficiency drop (Chen et al., 2017).

5.3. Indicated mean effective pressure

Figure 11 shows the indicated mean effective pressure values which were obtained from the simulations. Indicated mean effective pressure values decreased between 9.47% and 13.82% with using methane as fuel. According to the theoretical results for methane fuel, energy output value decreased per cycle and lower IMEP values were obtained due to lower heating value on volume basis and lower energy density per unit volume of methane gas.

5.4. Carbon monoxide

Air-fuel ratio is one of the most important parameter for carbon monoxide emissions. As mentioned earlier, simulations have been run at nearly stoichiometric air-fuel ratio condition for both petrol and methane fuel. Figure 12 shows the specific carbon monoxide emissions at different engine speeds, which were obtained from the theoretical model for petrol and methane fuels. While working with methane as fuel, there is a slight decrease at specific carbon monoxide emissions for all engine speeds. Maximum drop occurred as 5.42% with using methane fuel at 3650 rpm engine speed. Although in peak in-cylinder pressure and in-cylinder temperature values were reduced with using methane, the low C/H ratio of methane causes slight reduction in specific carbon monoxide emission values. As known that methane is the major component of CNG and Putrasari *et al.* (2015) claimed that lower C/H ratio causes lower carbon monoxide emission in their study with using CNG as fuel. Under these conditions, the lower carbon monoxide emissions with methane usage can be attributed to the lower C/H ratio and lower carbon content of methane fuel. Besides, local rich mixture regions and chemical equilibrium values due to macro mixture irregularities can be seen as a source of carbon monoxide generated as emissions.

5.5. Total unburned hydrocarbons

Specific total unburned HC (THC) emissions, which were acquired from different engine speeds for methane and petrols can be seen in Figure 13. It can be shown in the graph that specific THC emission values increased between 16.56% and 28.52% for all engine speeds with methane fuel simulation. The maximum rise in THC emission occurred at 3650 rpm engine speed and it increased from 1.40 g/kWh to 1.80 g/kWh that equals to 28.52% increase.

THC emissions are sensitive to many constructive factors (combustion chamber surface and volume ratio, blow-by effect, narrow volumes, etc.) and operating conditions (engine load, ignition advance, regime temperature, engine speed). When Figure 13 is examined, firstly THC emission drops as the engine speed increases due to improving macro scale mixture properties and flame extinction zones reduce by the help of increase in combustion chamber turbulence level (Szwaja et al., 2018). Combustion duration gets practically longer in terms of crank angle as the engine speed increases further. Thus, improvement rate of THC decreases due to insufficient time for combustion before the chamber volume expands. When engine speed exceeds a certain value, this effect becomes dominant and leads THC emissions to show increasing trend (Duc et al., 2019). Moreover, increase of both frictional and inertial losses with increasing engine speed cause more apparent increase in specific THC emissions in comparison to THC emissions in ppm (Suiuay et al., 2020). The THC results, which are seen in Figure 13, are in agreement with the studies of Duc et al. (2019) and Asfar and Al-Azzam (2001).

The quenching distance, which is the most important parameter for THC emission, is nearly same for both fuels (Pan et al., 2018). On the other hand, owing to low flame velocity of methane, maximum in-cylinder temperature values drop which is the main reason of high THC emission for methane simulations.

5.6. Nitrous oxides

Oxides of nitrogen emissions, which need high cost after treatment systems, are very harmful for human health (Wang et al., 2018). It is very important to take under control NO_x emissions which are emitted from internal combustion engines. Specific NO_x emissions at different engine speeds for petrol and methane fuel are shown in Figure 14. In this study, specific NO_x emissions decreased from 1.54 g/kWh to 1.39 g/kWh at 2650 rpm engine speed. Similarly nitrogen oxides emission values decreased from 1.40 g/kWh to 1.24 g/kWh at 2900 rpm, from 1.32 g/kWh to 1.15 g/kWh at 3150 rpm, from 1.22 g/kWh to 1.06 g/kWh at 3400 rpm and from 1.16 g/kWh to 0.99 g/kWh at 3650 rpm engine speed with using methane fuel. The reduction in specific NO_x emissions at 2650, 2900, 3150, 3400 and 3650 rpm engine speeds with using methane as fuel were 9.41%, 11.36%, 13.10%, 12.76% and 14.72%, respectively.

The NO_x emissions are largely dependent on in-cylinder temperature values (Guardiola et al., 2017). Hence, low maximum pressure and temperature values due to low flame speed (Di Iorio, Sementa and Vaglieco, 2016) and low energy content of methane, explain dramatic decrease in NO_x emissions.

6. Conclusion

On the performed study, the comparison of petrol and methane fuels were investigated at full engine load, stoichiometric condition and different engine speeds (2650 rpm to 3650 rpm). Firstly, SI engine was experimentally tested and performance, emission values and combustion characteristics were obtained with petrol at 2650 rpm and 3400 rpm engine speeds, with methane at 3400 rpm engine speed. Secondly, theoretical model was developed and validated with the petrol and methane fuelled experimental results. Lastly, methane and petrol SI engine simulations were compared each other and obtained results are summa*rise*d as given below.

- Maximum in-cylinder pressure and maximum normalized heat release rate values were decreased up to 8.8% and 9.4%, respectively with using methane as fuel in the SI engine. The reason is that methane has lower energy density, lower flame velocity and lower energy content on volume basis than petrol.
- ITE and IMEP values were reduced up to 12.1% and 13.82%, respectively with using methane. This is because methane has low flame velocity and low LHV on volume basis.
- Carbon monoxide emissions slightly improved (up to 5.4%) with using methane. The reason is low C/H ratio of methane fuel. However, a dramatic increase (up to 28.5%) in THC emissions weren't prevented. This is because methane has lower flame velocity than petrol. An unprecedented improvement (up to 14.7%) was obtained in NO_x emissions. The reason is that low in-cylinder pressure and low in-cylinder temperature values obtained during methane fuelled SI engine operation.
- Today, CNG, LNG use in public transportation buses and LPG in passenger cars are becoming widespread. Provided that the applicable conditions are met, the advantage performance will become prominent, owing to higher thermal capacity of methane. At the same time, compared to liquid fuels, the mixture provides a great deal of homogeneity because it is injected in the gas phase. Thus, liquid inertia, evaporation process and other factors, that worsen the macro scale mixture formation, are eliminated and a more homogeneous mixture can be obtained.

- In future studies it will be useful to examine the post-combustion emission reduction methods for methane and petrol operating conditions. Due to different combustion performances and different values of the chemical composition and the temperature of the exhaust gas due to their thermal values, studies aiming to optimize the current performance and performance of the closed-loop three-way catalytic converters for changing fuel conditions will contribute to a strong alternative to conventional fuels.
-

Acknowledgement

This research was supported by Tubitak (Scientific and Technological Research Council of Turkey) with 1512 project. Project Number: 2150175. The authors are also indebted to Şahin Metal A.Ş. and Erin Motor for providing us with test apparatus and equipment donation. The second author of the manuscript has been financially supported by TUBITAK 2228-B program.

Accepted manuscript doi: 10.1680/jener.19.00055

Notation

BSFC	brake specific fuel consumption
BTE	brake thermal efficiency
CA	crank angle
CNG	compressed natural gas
HC	hydrocarbon
HRR	heat release rate
IMEP	indicated mean effective pressure
ITE	indicated thermal efficiency
LHV	lower heating value
NO_x	oxides of nitrogen
RPM	revolutions per minute
SI	spark ignition
THC	total unburned hydrocarbons

V	is instant cylinder volume (m^3) calculated in Equation 1
V_H	is cylinder displacement (m^3)
λ	is ratio of crank radius to connecting rod length
α	is crank angle (degree)
ε	is compression ratio of the engine
W_i	is indicated work of the engine per cycle (J)
P_{mi}	is mean indicated pressure (Pa)
P	is measured in-cylinder pressure (Pa)
N_i	is indicated engine power (kW)
n	is engine speed (rpm)

Accepted manuscript doi: 10.1680/jener.19.00055

ITE is indicated thermal efficiency

$\dot{m}_f$ is mass flow rates of fuels (petrol or methane) (kg/s)

LHV_f is lower heating values of fuels (petrol or methane) (kJ/kg).

$\dot{Q}$ is heat release rate (HRR) (J/^{o}CA) and k is working mixture polytrophic index.

Q is total fuel heat input

α_0 is crank angle at the beginning of combustion

$\Delta\alpha_c$ is combustion duration

m is shape parameter

a is Vibe parameter which is equal to 6.9 for complete combustion

$\dot{m}_{exh}$ and $\dot{m}_{int}$ is mass flow rates of exhaust gases and intake air, respectively (g/h)

EP_i is specific emission value of relevant gases (g/kWh)

EV_i is relevant gases amount in proportion to total exhaust gases (by volume for carbon monoxide and by particle count for THC and NO_x)

M_i and M_{exh} are molar mass of relevant gases and exhaust gases respectively (kg/kmol).

$(W_R)_{P,B}$ denotes the propagated uncertainty for either precision error $(W_R)_P$, or systematic (Bias) error $(W_R)_B$ functions

$x_1, x_2, \ldots, x_n$ are the measured variables

$w_1, w_2, \ldots w_n$ are the corresponding uncertainties of the variables

Accepted manuscript doi: 10.1680/jener.19.00055

References

Akansu, S. O., Kahraman, N., and Çeper, B. (2007). Experimental study on a spark ignition engine fuelled by methane–hydrogen mixtures. *International Journal of Hydrogen Energy*, *32*(17), 4279-4284.

Amirante, R., Distaso, E., Di Iorio, S., Sementa, P., Tamburrano, P., Vaglieco, B. M., and Reitz, R. D. (2017). Effects of natural gas composition on performance and regulated, greenhouse gas and particulate emissions in spark-ignition engines. *Energy Conversion and Management*, *143*, 338-347.

Asfar, K. R., and Al-Azzam, R. (2001). Engine performance using vaporizing carburetor. Energy conversion and management, 42(6), 755-761.

AVL LIST GmbH. (2013). Theory AVL BOOST v2013.2. Edition 11/2013. Graz: AVL LIST GmbH.

Bauer, C. G., and Forest, T. W. (2001). Effect of hydrogen addition on the performance of methane-fueled vehicles. Part I: effect on SI engine performance. *International Journal of Hydrogen Energy*, *26*(1), 55-70.

Chen, Z., Zhang, F., Xu, B., Zhang, Q., and Liu, J. (2017). Influence of methane content on a LNG heavy-duty engine with high compression ratio. *Energy*, *128*, 329-336.

Costagliola, M. A., Prati, M. V., Florio, S., Scorletti, P., Terna, D., Iodice, P., Buono, D., Senatore A. (2016). Performances and emissions of a 4-stroke motor cycle fuelled with ethanol/gasoline blends. *Fuel*, 183, 470-477.

Deng, B., Fu, J., Zhang, D., Yang, J., Feng, R., Liu, J., ... and Liu, X. (2013). The heat release analysis of bio-butanol/gasoline blends on a high speed SI (spark ignition) engine. *Energy*, *60*, 230-241.

Di Iorio, S., Sementa, P., and Vaglieco, B. M. (2016). Analysis of combustion of methane and hydrogen–methane blends in small DI SI (direct injection spark ignition) engine using advanced diagnostics. *Energy, 108,* 99-107.

Duc, K. N., Duy, V. N., Hoang-Dinh, L., Viet, T. N., and Le-Anh, T. (2019). Performance and emission characteristics of a port fuel injected, spark ignition engine fuelled by compressed natural gas. Sustainable Energy Technologies and Assessments, 31, 383-389.

EEA. (2016a). *Air Quality in Europe*. Report No 28/2016. Copenhagen: EEA.

EEA. (2016b). *Electric vehicles in Europe*. Report No 20/2016. Copenhagen: EEA.

EEA. (2017). *Monitoring CO2 emissions from new passenger cars and vans in 2016*. Report No 19/2017. Copenhagen: EEA.

Egnell, R. (1998). Combustion diagnostics by means of multizone heat release analysis and NO calculation. *SAE transactions*, 691-710.

Environment Pollution (Prevention and Control) Authority for the National Capital Region. (2017). Comprehensive Action Plan for air pollution control. Report No. 70. Delhi: EPCA.

Geo, V. E., Godwin, D. J., Thiyagarajan, S., Saravanan, C. G., and Aloui, F. (2019). Effect of higher and lower order alcohol blending with gasoline on performance, emission and combustion characteristics of SI engine. *Fuel*, *256*, 115806.

Gharehghani, A., Hosseini, R., Mirsalim, M., and Yusaf, T. F. (2015). A comparative study on the first and second law analysis and performance characteristics of a spark ignition engine using either natural gas or gasoline. *Fuel*, *158*, 488-493.

Guardiola, C., Martín, J., Pla, B., and Bares, P. (2017). Cycle by cycle NOx model for diesel engine control. *Applied Thermal Engineering*, *110*, 1011-1020.

Gupta, A., and Abdel-Gayed, R. (2015). Qualitative governing approach of a spark ignition engine using exhaust gas recirculation. *Energy Procedia*, *66*, 97-100

Heywood JB. (1988). Internal combustion engine fundamental. New York: McGraw-Hill, Inc.

Hu, M., Huang, W., Cai, J., and Chen, J. (2017). The evaluation on liquefied natural gas truck promotion in Shenzhen freight. *Advances in Mechanical Engineering*, *9*(6), 1687814017705065.

Iodice, P., Langella, G., Amoresano, A. (2018). Ethanol in gasoline fuel blends: Effect on fuel consumption and engine out emissions of SI engines in cold operating conditions. *Applied Thermal Engineering*, 130, 1081-1089.

Iodice, P., Senatore, A. (2016). Atmospheric pollution from point and diffuse sources in a National Interest Priority Site located in Italy. *Energy& Environment*, 27(5), 586-596.

Irimescu, A. (2013). Comparison of combustion characteristics and heat loss for gasoline and methane fueling of a spark ignition engine. *Proceedings of the Romanian Academy, Series A*, *14(2)*, 161-168

Irimescu, A., Vasiu, G., and Tordai, G. T. (2014). Performance and emissions of a small scale generator powered by a spark ignition engine with adaptive fuel injection control. *Applied energy*, *121*, 196-206.

İlhak, M. İ., Doğan, R., Akansu, S. O., and Kahraman, N. (2020). Experimental study on an SI engine fueled by gasoline, ethanol and acetylene at partial loads. *Fuel*, *261*, 116148.

Kline, S. J., and McClintock, F. A. (1953). Describing Uncertainties in Single-Sample Experiments, *Mechanical Engineering, Vol. 75.*

Lyu, M., Zhang, C., Bao, X., Song, J., and Liu, Z. (2017). Effects of the substitution rate of natural gas on the combustion and emission characteristics in a dual-fuel engine under full load. *Advances in Mechanical Engineering*, *9*(12), 1687814017747158.

Montoya, J. P. G., Amell, A. A., and Olsen, D. B. (2016). Prediction and measurement of the critical compression ratio and methane number for blends of biogas with methane, propane and hydrogen. *Fuel*, *186*, 168-175.

Moreno, F., Muñoz, M., Arroyo, J., Magén, O., Monné, C., and Suelves, I. (2012). Efficiency and emissions in a vehicle spark ignition engine fueled with hydrogen and methane blends. *International Journal of Hydrogen Energy*, *37*(15), 11495-11503.

Pan, J., Li, N., Wei, H., Hua, J., and Shu, G. (2018). Experimental investigations on combustion acceleration behavior of methane/gasoline under partial load conditions of SI engines. *Applied Thermal Engineering*, 139, 432–444

Putrasari, Y., Praptijanto, A., Nur, A., Wahono, B., and Santoso, W. B. (2015). Evaluation of performance and emission of SI engine fuelled with CNG at low and high load condition. *Energy Procedia*, *68*, 147-156.

Rimkus, A., Žaglinskis, J., Rapalis, P., and Skačkauskas, P. (2015). Research on the combustion, energy and emission parameters of diesel fuel and a biomass-to-liquid (BTL) fuel blend in a compression-ignition engine. *Energy Conversion and Management*, *106*, 1109-1117.

Sjerić, M., Taritaš, I., Tomić, R., Blažić, M., Kozarac, D., and Lulić, Z. (2016). Efficiency improvement of a spark-ignition engine at full load conditions using exhaust gas recirculation and variable geometry turbocharger–Numerical study. *Energy conversion and management*, *125*, 26-39.

Subramanian, K. A., Mathad, V. C., Vijay, V. K., and Subbarao, P. M. V. (2013). Comparative evaluation of emission and fuel economy of an automotive spark ignition vehicle fuelled with methane enriched biogas and CNG using chassis dynamometer. *Applied Energy*, *105*, 17-29.

Suiuay, C., Laloon, K., Katekaew, S., Senawong, K., Noisuwan, P., and Sudajan, S. (2020). Effect of gasoline-like fuel obtained from hard-resin of Yang (Dipterocarpus alatus) on single cylinder gasoline engine performance and exhaust emissions. Renewable Energy, 153, 634-645.

Szwaja, S., Ansari, E., Rao, S., Szwaja, M., Grab-Rogalinski, K., Naber, J. D., and Pyrc, M. (2018). Influence of exhaust residuals on combustion phases, exhaust toxic emission and fuel consumption from a natural gas fuelled spark-ignition engine. Energy Conversion and Management, 165, 440-446.

Tahir, M. M., Ali, M. S., Salim, M. A., Bakar, R. A., Fudhail, A. M., Hassan, M. Z., and Muhaimin, M. A. (2015). Performance analysis of a spark ignition engine using compressed natural gas (CNG) as fuel. *Energy Procedia*, *68*, 355-362.

Thurnheer, T., Soltic, P., and Eggenschwiler, P. D. (2009). SI engine fuelled with gasoline, methane and methane/hydrogen blends: heat release and loss analysis. *International Journal of Hydrogen Energy*, *34*(5), 2494-2503.

Transport for London. (2016). *Taxi and Private Hire Action Plan*. London: Transport for London.

VDMA Engines and Systems. (2017). Exhaust Emission Legislation Diesel- and Gas engines. Frankfurt: VDMA.

Wang, Z. X., Wang, L. W., Gao, P., Yu, Y., and Wang, R. Z. (2018). Analysis of composite sorbents for ammonia storage to eliminate NOx emission at low temperatures. *Applied Thermal Engineering*, *128*, 1382-1390.

Yu, X., Li, G., Dong, W., Shang, Z., Guo, Z., Li, Y., ... and Zhao, Z. (2020). Numerical study on effects of hydrogen direct injection on hydrogen mixture distribution, combustion and emissions of a gasoline/hydrogen SI engine under lean burn condition. *International Journal of Hydrogen Energy*, *45*(3), 2341-2350.

Table 1. Properties comparison of petrol and methane (Pan et al., 2018)

Parameter	Petrol	Methane
Formula	C_4-C_{12}	methane
C/H ratio (%)	0.56	0.25
Molecular weight (kg/kmole)	98	16
Density of standard conditions (kg/m^3)	720	0.67
Auto-ignition temperature (^{o}C)	350	540
Research octane number	92	125
Stoichiometric air-fuel ratio	14.6	17.24
Quenching distance (mm)	2.02	2.03
Flammability limit (vol %)	5.3/14	1.4/7.6
Laminar burning velocity (m/s)	0.45	0.43

Table 2. Engine specifications and dynamometer features

Engine specifications	
Engine manufacturer	Honda
Number of cylinders	1
Compression ratio	8.5:1
Cooling	Air
Bore × stroke [mm]	77 × 58
Cylinder volume [cm^3]	270
Net power [kW]	6.3 / 3600 rpm
Recommended speed range [rpm]	2000-3500
Aspiration	Natural
Dynamometer Features	
Power [kVA] [kW]	8

Accepted manuscript doi:
10.1680/jener.19.00055

Table 3. Petrol fuelled model validation parameters and error values

Parameter	Experimental (2650/3400 rpm)	Simulation	Error [%]
Maximum pressure [bar]	36.11 / 28.35	35.17 / 27.46	2.6 / 3.1
ITE [%]	25.25 / 21.94	25.04 / 21.69	0.82 / 1.16
IMEP [bar]	9.46 / 8.88	9.55 / 8.76	-0.99 / 1.31
Carbon monoxide [g/kWh]	933 / 1309	941 / 1282	-0.86 / 2.06
THC [g/kWh]	1.44 / 1.16	1.51 / 1.26	-4.78 / -8.60
NO_X [g/kWh]	1.55 / 1.20	1.54 / 1.22	1.05 / -1.76

Table 4. Methane fuelled model validation parameters and error values

Parameter	Experimental	Simulation	Error [%]
Maximum pressure [bar]	27.35	26.52	3.0
ITE [%]	19.98	19.68	1.48
IMEP [bar]	7.81	7.93	-1.58
Carbon monoxide [g/kWh]	1254	1232	1.74
THC [g/kWh]	1.49	1.57	-5.12
NO_X [g/kWh]	1.08	1.06	2.21

Table 5. Measurement accuracies and the calculated uncertainties.

Parameter	Device	Accuracy
Engine speed	Incremental encoder	±5 rpm
In-cylinder pressure	Kistler 6118B	±0.3 bar
Petrol flow rate	Biotech VZS-005	±1 % (of reading)
Methane flow rate	New-Flow TLF	±1 % (F.S.)
Carbon monoxide	AVL Digas 4000	0.01 % Vol.
THC	AVL Digas 4000	1 ppm
NO_x	AVL Digas 4000	1 ppm
Calculated results		Uncertainty value
Indicated specific energy consumption		±0.68 ÷ 0.79 %

Accepted manuscript doi: 10.1680/jener.19.00055

Figure captions

Figure 1. Schematic explanation of the experimental setup

Figure 2. View of AVL Boost single-cylinder mathematical engine model

Figure 3. In-cylinder pressure variations of experimental and theoretical data at 2650 rpm engine speed with petrol

Figure 4. Normalised heat release variations of experimental and theoretical data at 2650 rpm engine speed with petrol

Figure 5. In-cylinder pressure variations of experimental and theoretical data at 3400 rpm engine speed with petrol

Figure 6. Normalised heat release variations of experimental and theoretical data at 3400 rpm engine speed with petrol

Figure 7. In-cylinder pressure variations of experimental and theoretical data at 3400 rpm engine speed with methane fuel

Figure 8. In-cylinder pressure variation comparisons of petrol and methane in different engine speeds (a) 2650 rpm, b) 2900 rpm, c) 3150 rpm, d) 3400 rpm, e) 3650 rpm

Figure 9. Normalised heat release rate variation comparisons of petrol and methane in different engine speeds (a) 2650 rpm, b) 2900 rpm, c) 3150 rpm, d) 3400 rpm, e) 3650 rpm

Figure 10. Comparisons of indicated thermal efficiency of petrol and methane

Figure 11. Comparisons of indicated mean effective pressure of petrol and methane

Figure 12. Specific carbon monoxide emission comparisons of petrol and methane

Figure 13. Specific THC emissions comparisons of petrol and methane

Figure 14. Specific NO_x emissions comparisons of petrol and methane

Accepted manuscript doi:
10.1680/jener.19.00055

Accepted manuscript doi:
10.1680/jener.19.00055

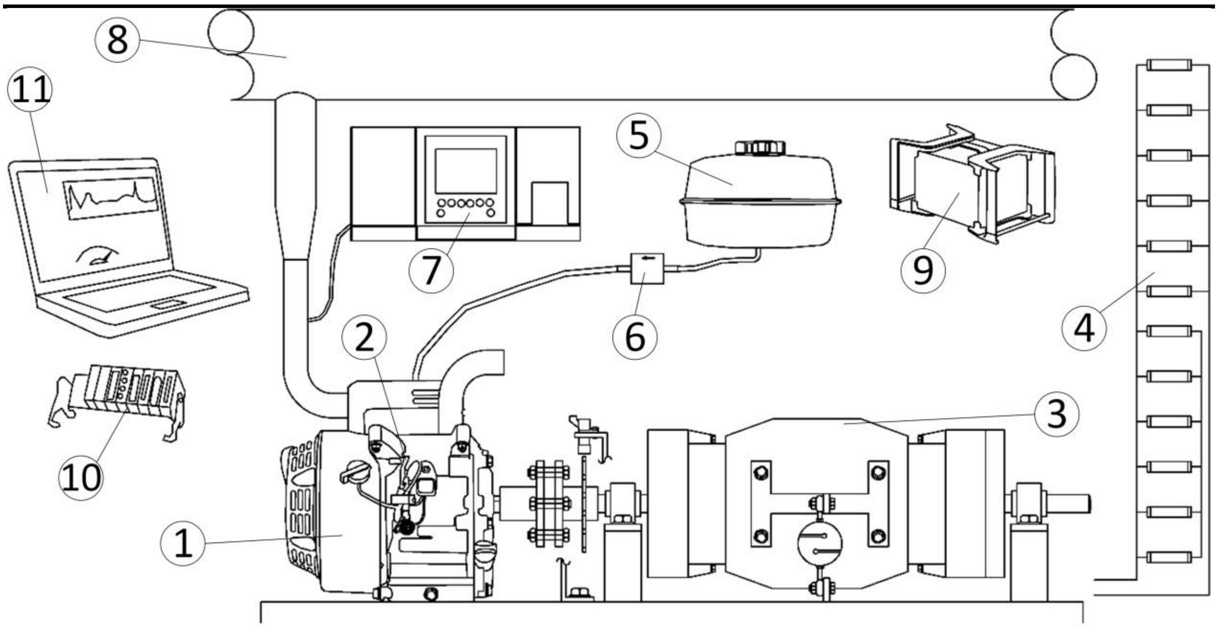

1. Test engine **2.** Pressure sensor **3.** Dynamometer **4.** External resistive load banks **5.** Gasoline tank **6.** Gasoline flowmeter **7.** Exhaust gas analyser **8.** Exhaust ventilation system **9.** KiBox combustion analyser **10.** NI data acquisition analyser **11.** Personal comuper for data recording and post processing

1-Schematic

Accepted manuscript doi:
10.1680/jener.19.00055

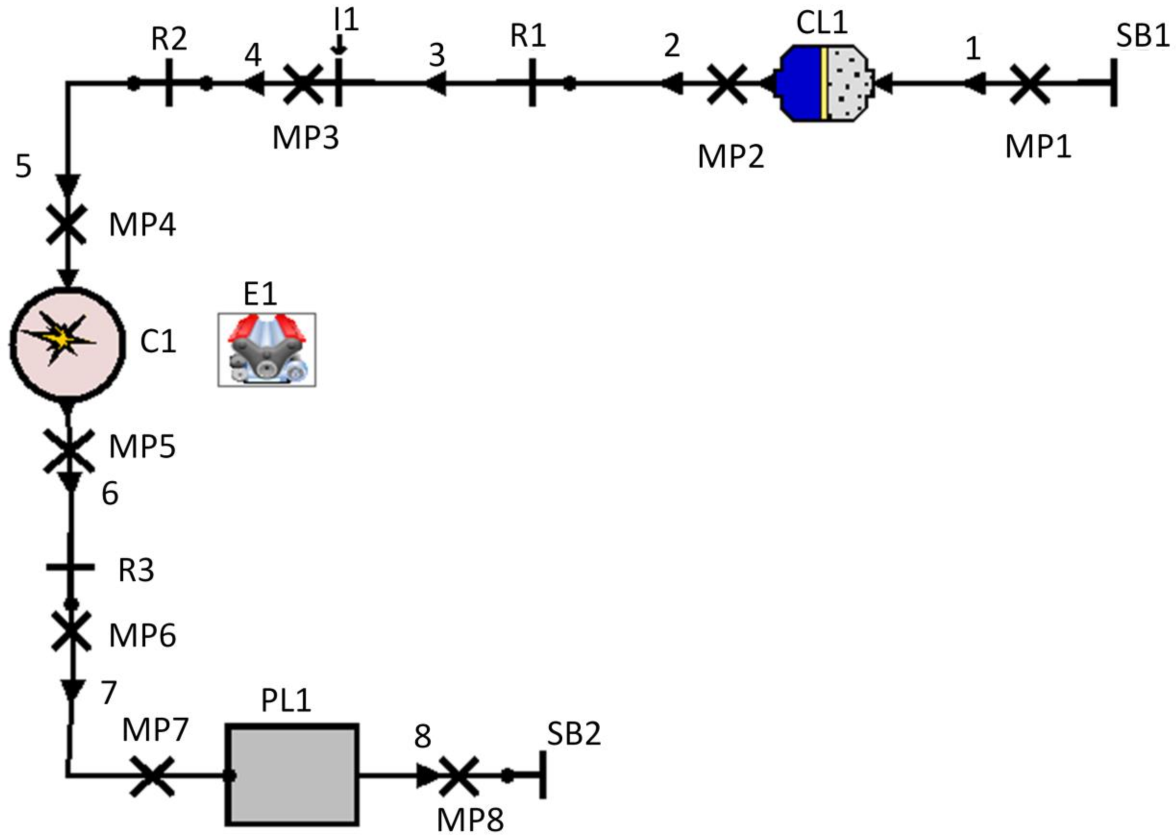

2-AVL Model

Accepted manuscript doi:
10.1680/jener.19.00055

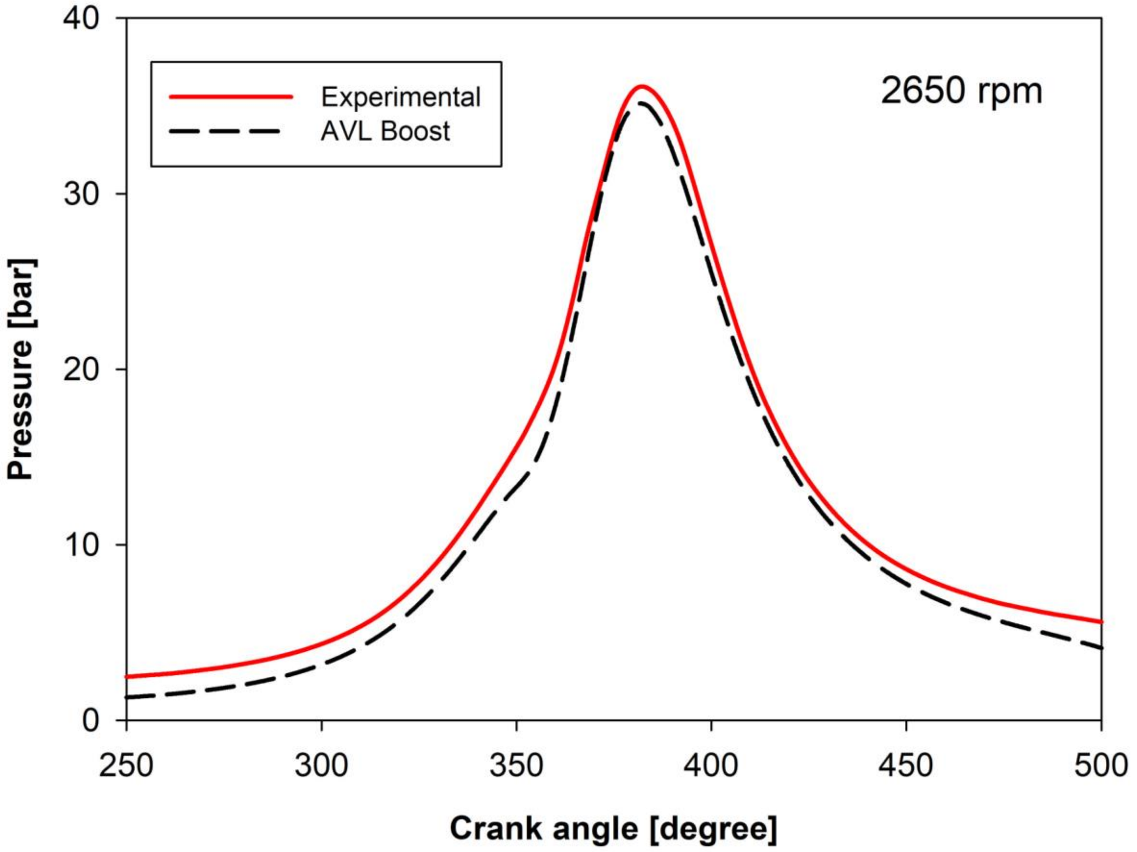

3-Gas_AVL-Exp_Pres2650

Accepted manuscript doi: 10.1680/jener.19.00055

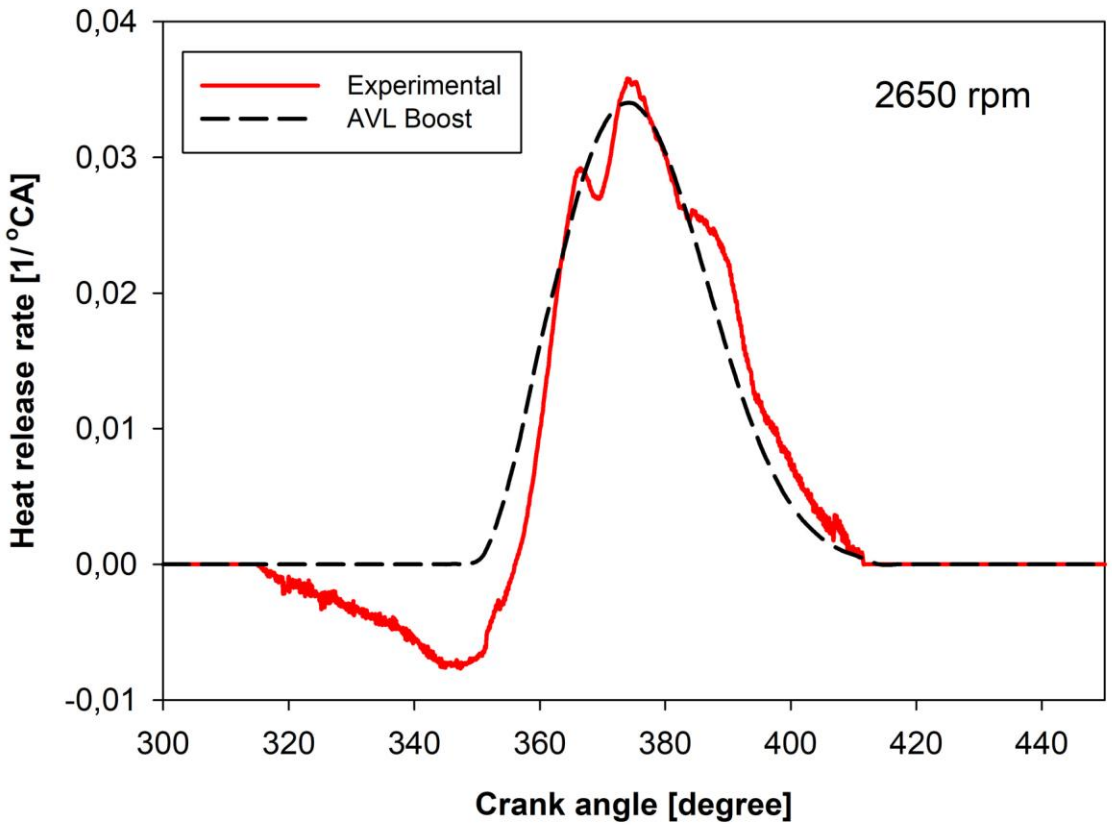

4-Gas_AVL-Exp_HRR2650

Accepted manuscript doi:
10.1680/jener.19.00055

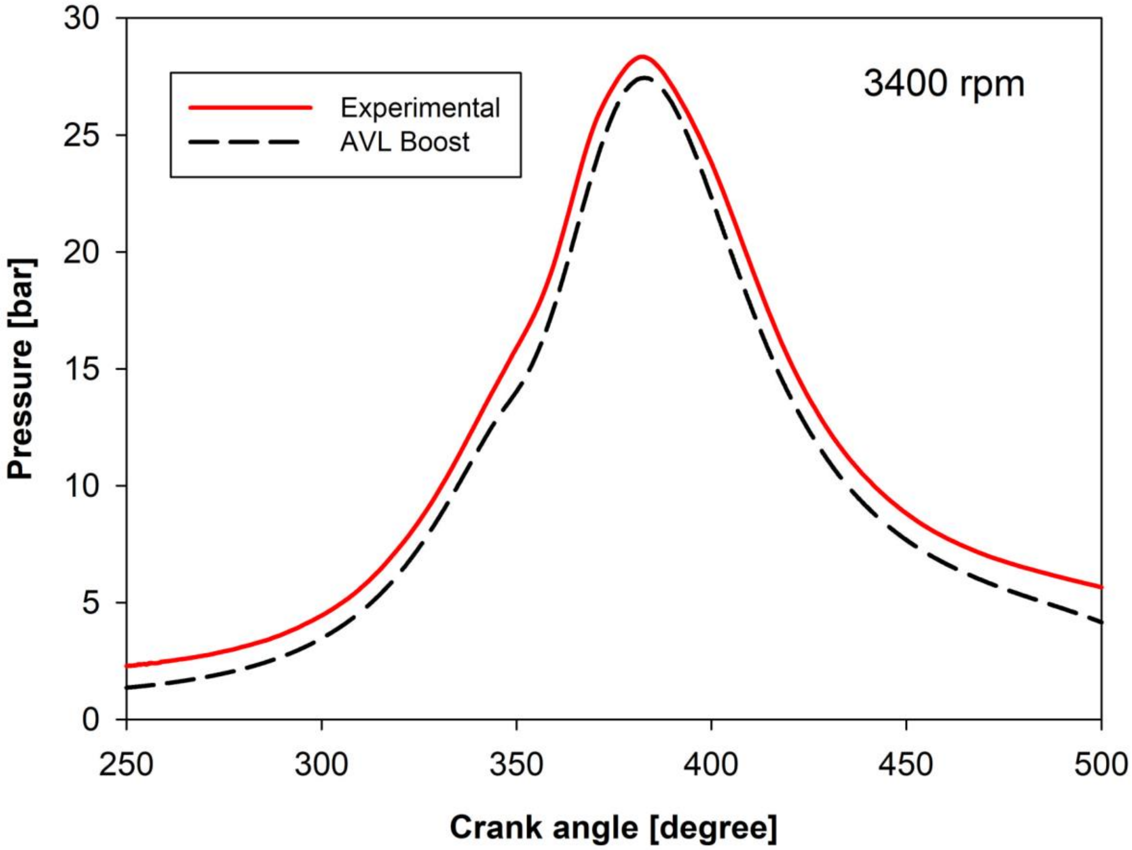

5-Gas_AVL-Exp_Pres3400

Accepted manuscript doi:
10.1680/jener.19.00055

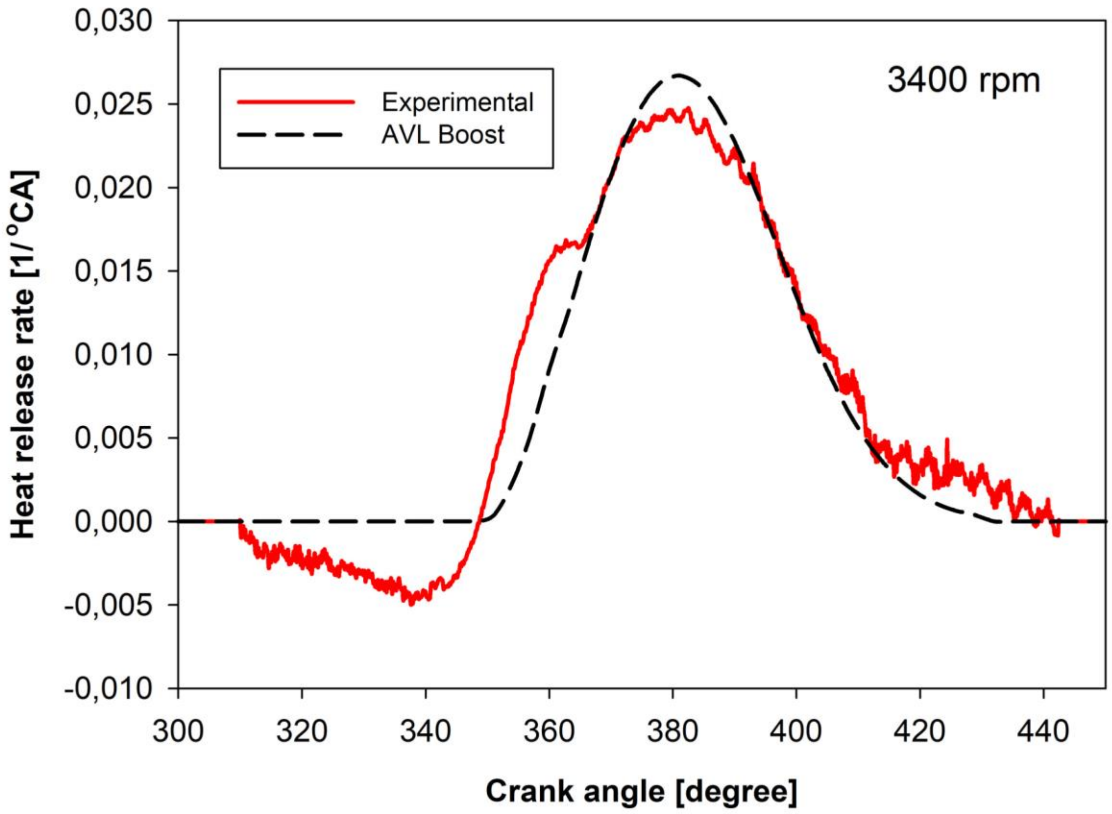

6-Gas_AVL-Exp_HRR3400

Accepted manuscript doi:
10.1680/jener.19.00055

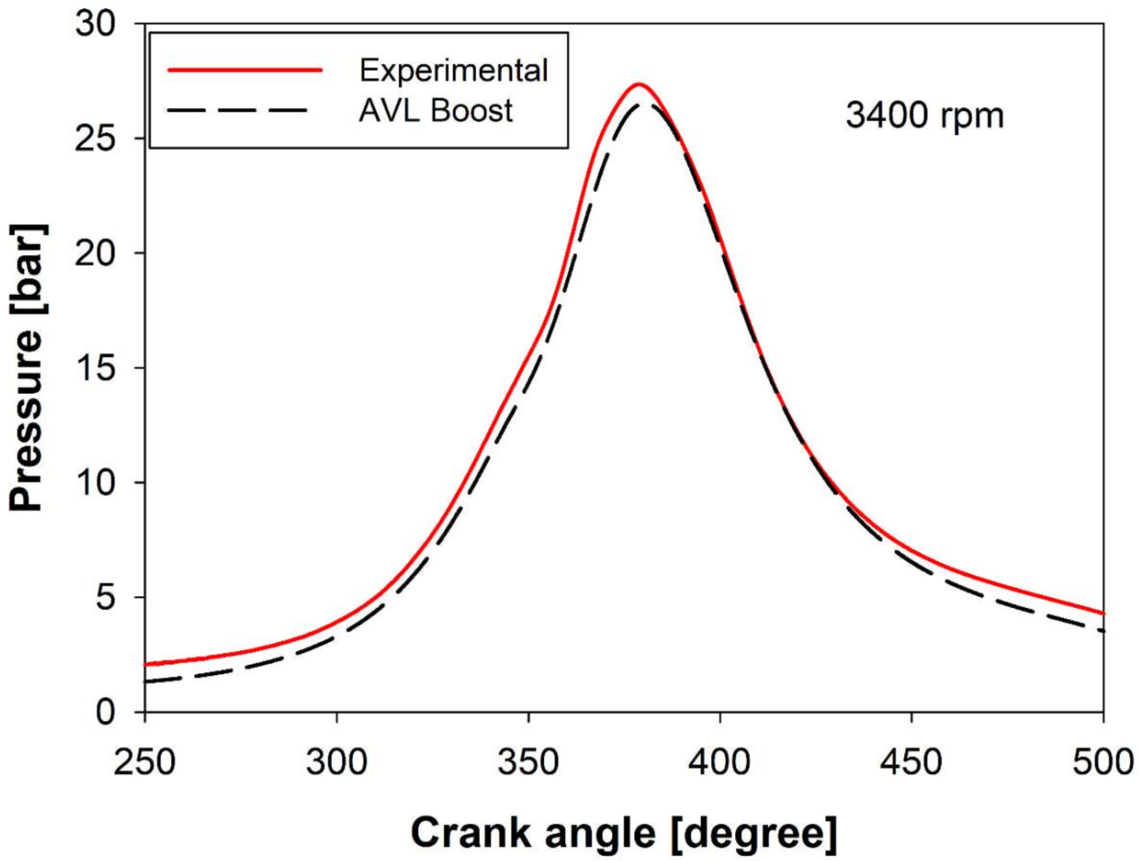

7-Met_AVL-Exp_Pres3400

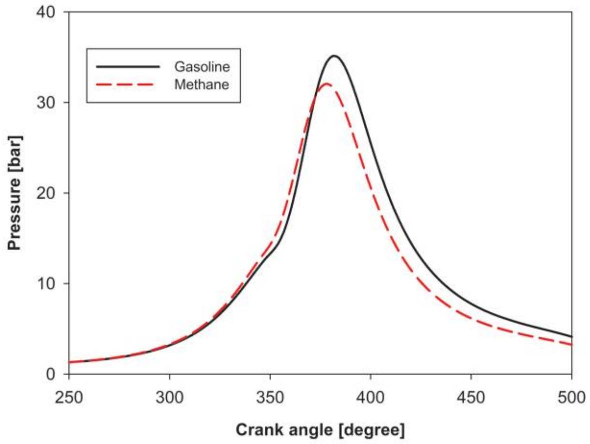

8a_Pres2650

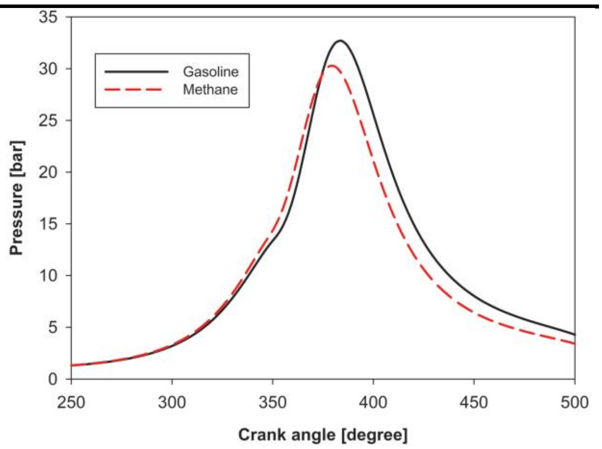

8b_Pres2900

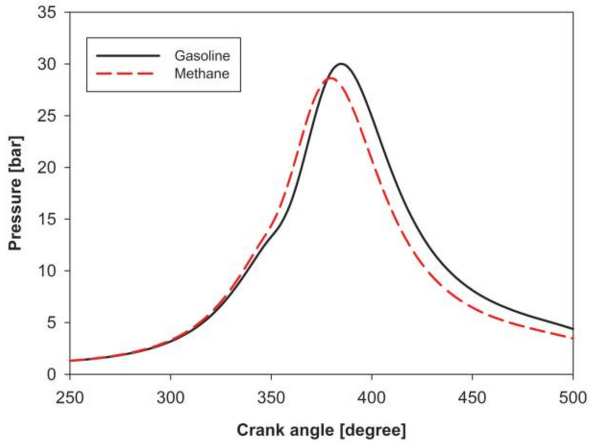

8c_Pres3150

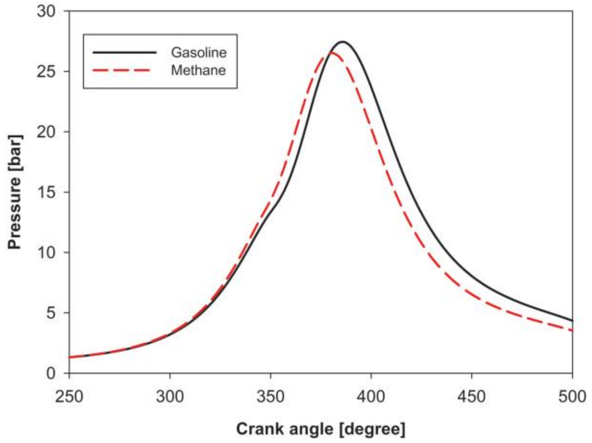

8d_Pres3400

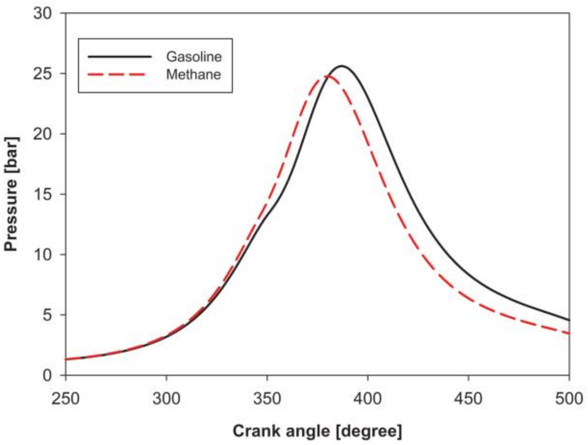

8e_Pres3650

Accepted manuscript doi: 10.1680/jener.19.00055

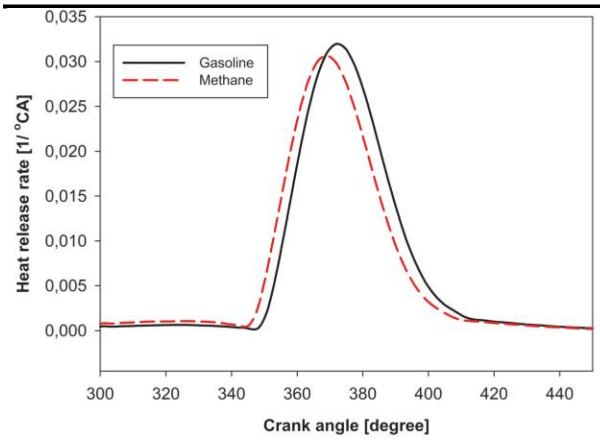

9a_HRR2650

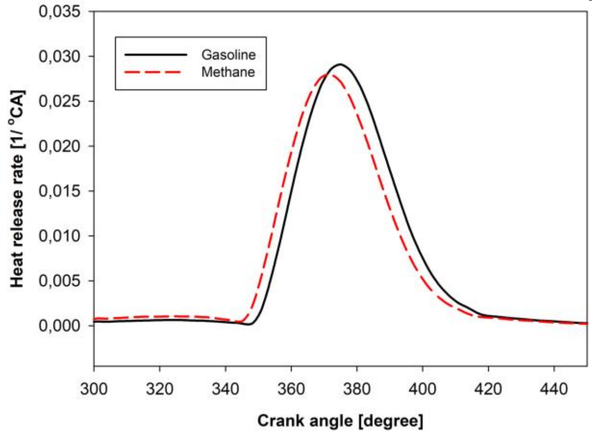

9b_HRR2900

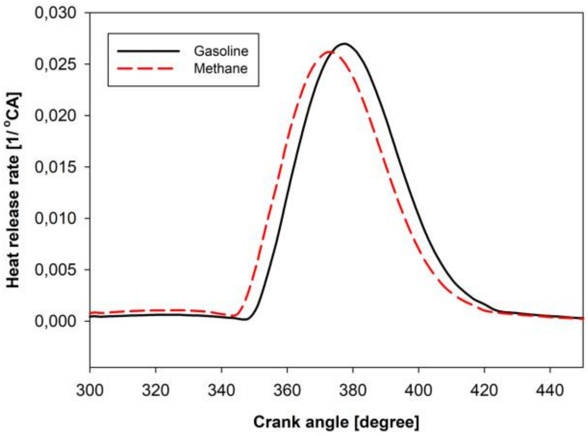

9c_HRR3150

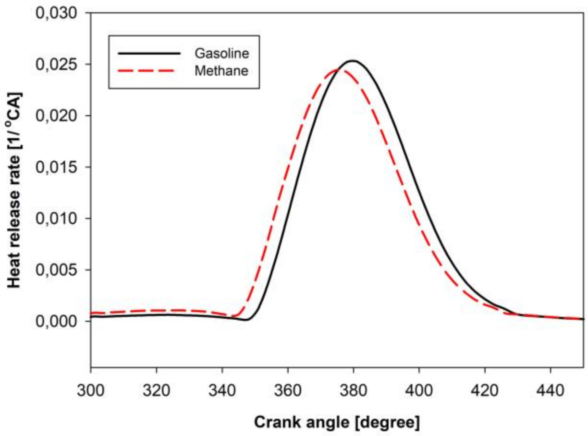

9d_HRR3400

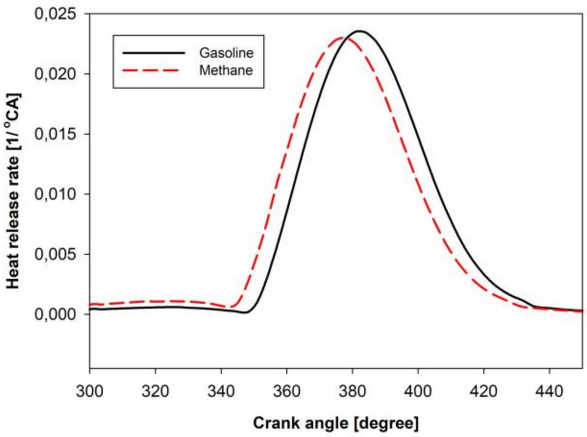

9e_HRR3650

Accepted manuscript doi:
10.1680/jener.19.00055

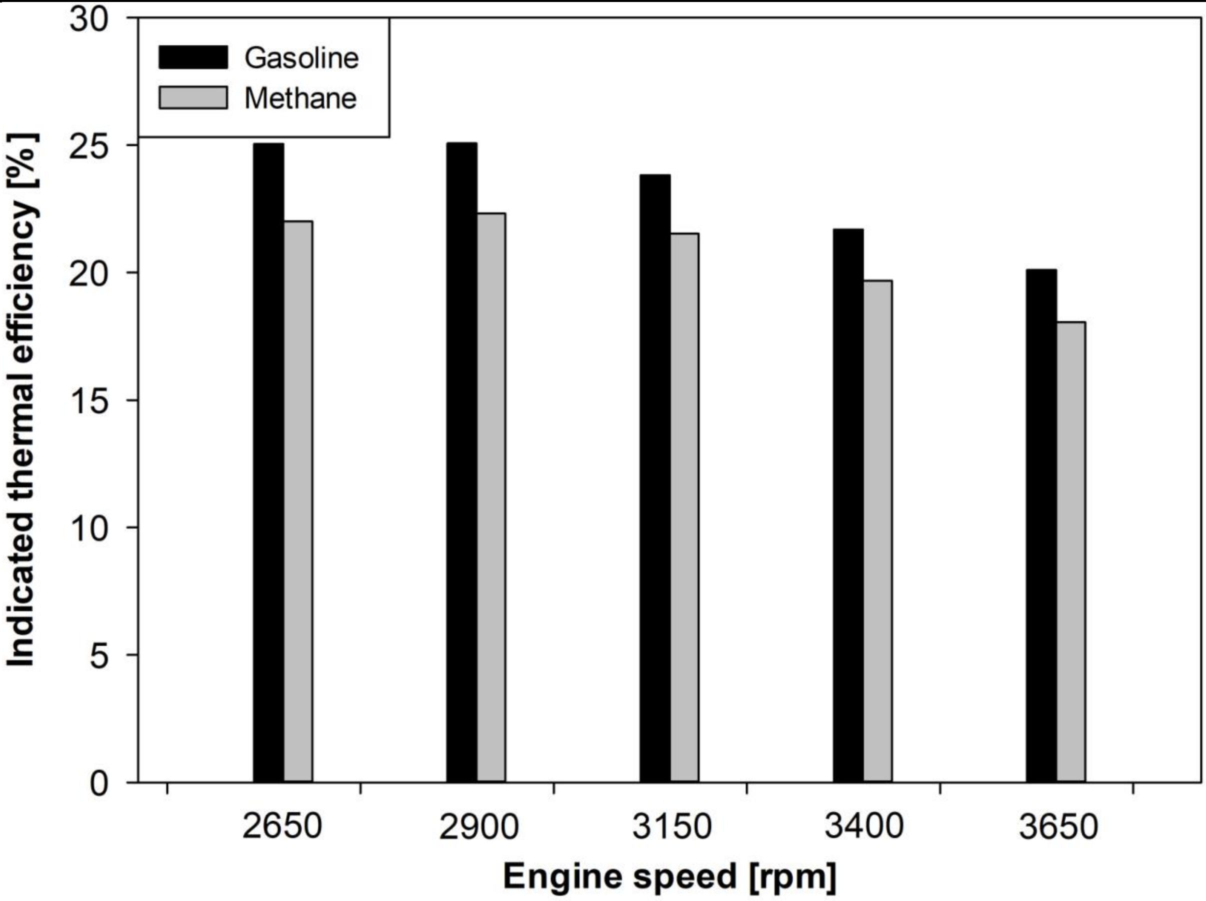

10-eta_i

Accepted manuscript doi:
10.1680/jener.19.00055

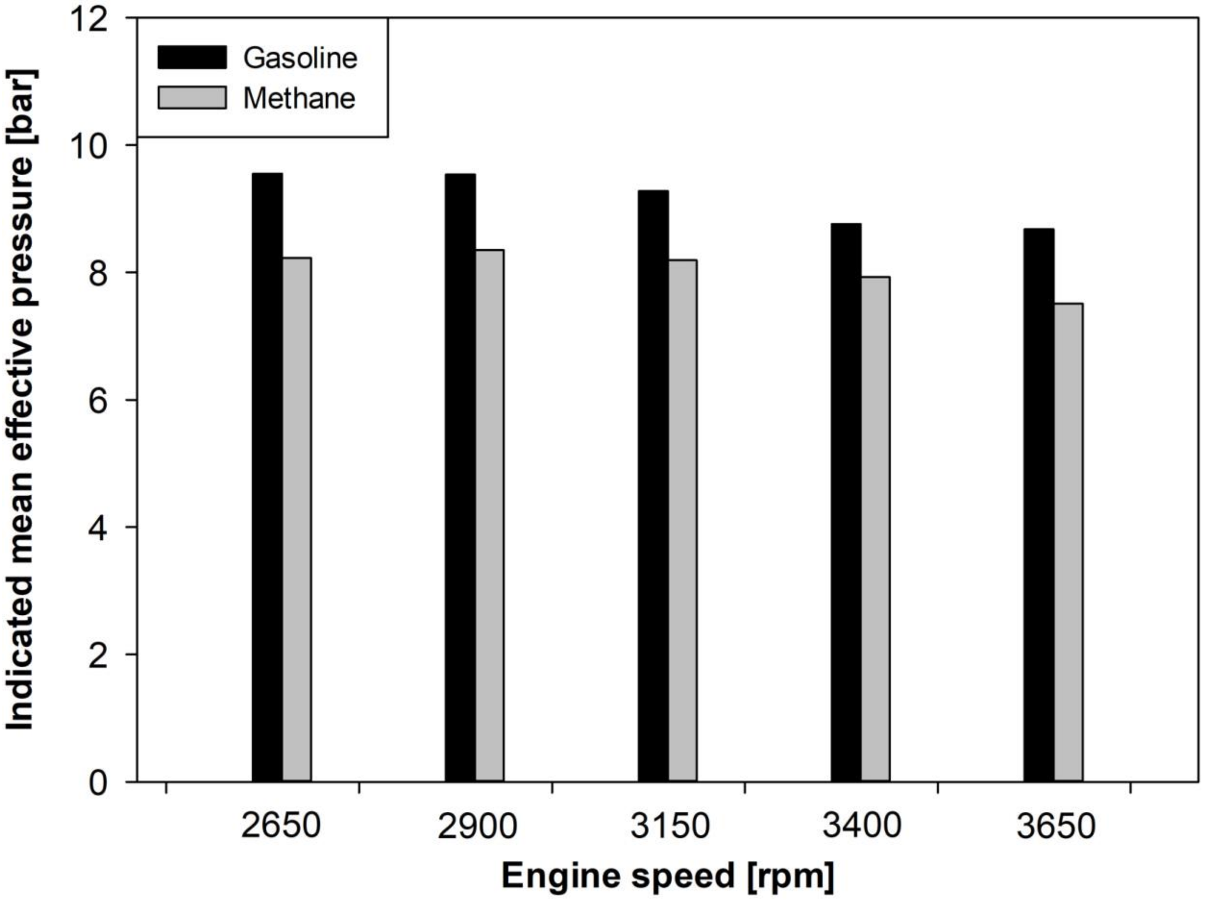

11-IMEP

Accepted manuscript doi:
10.1680/jener.19.00055

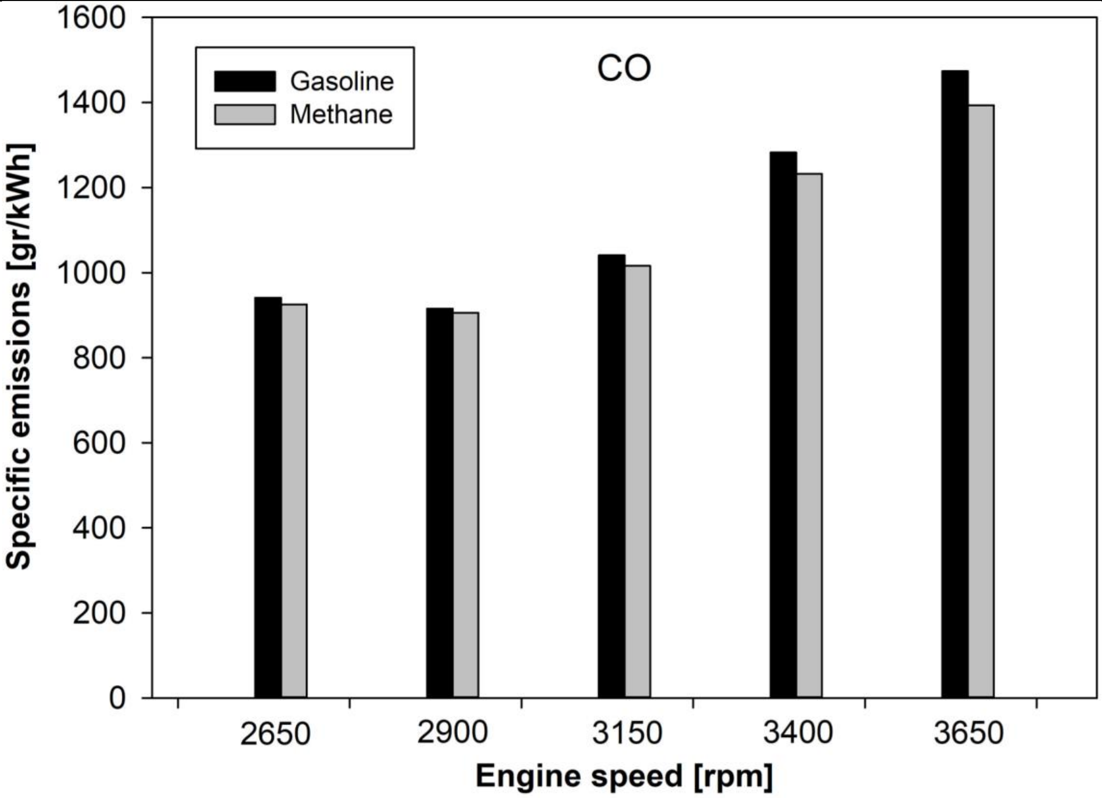

12-CO

Accepted manuscript doi:
10.1680/jener.19.00055

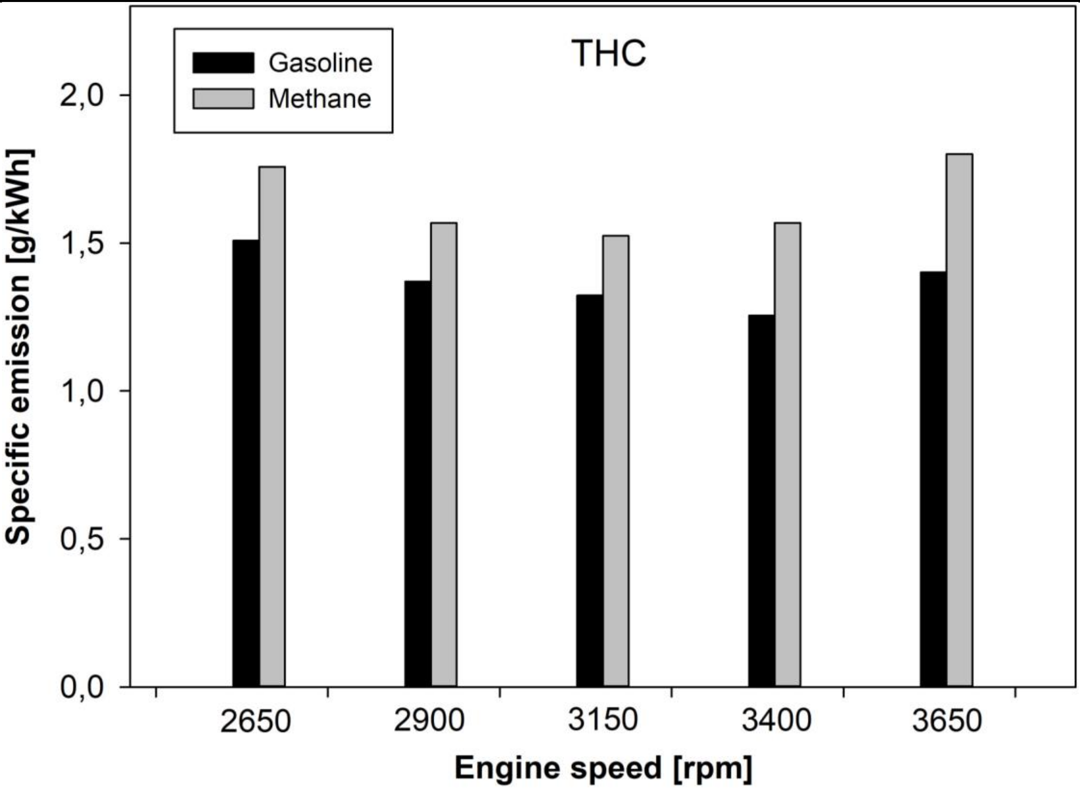

13-THC

Accepted manuscript doi:
10.1680/jener.19.00055

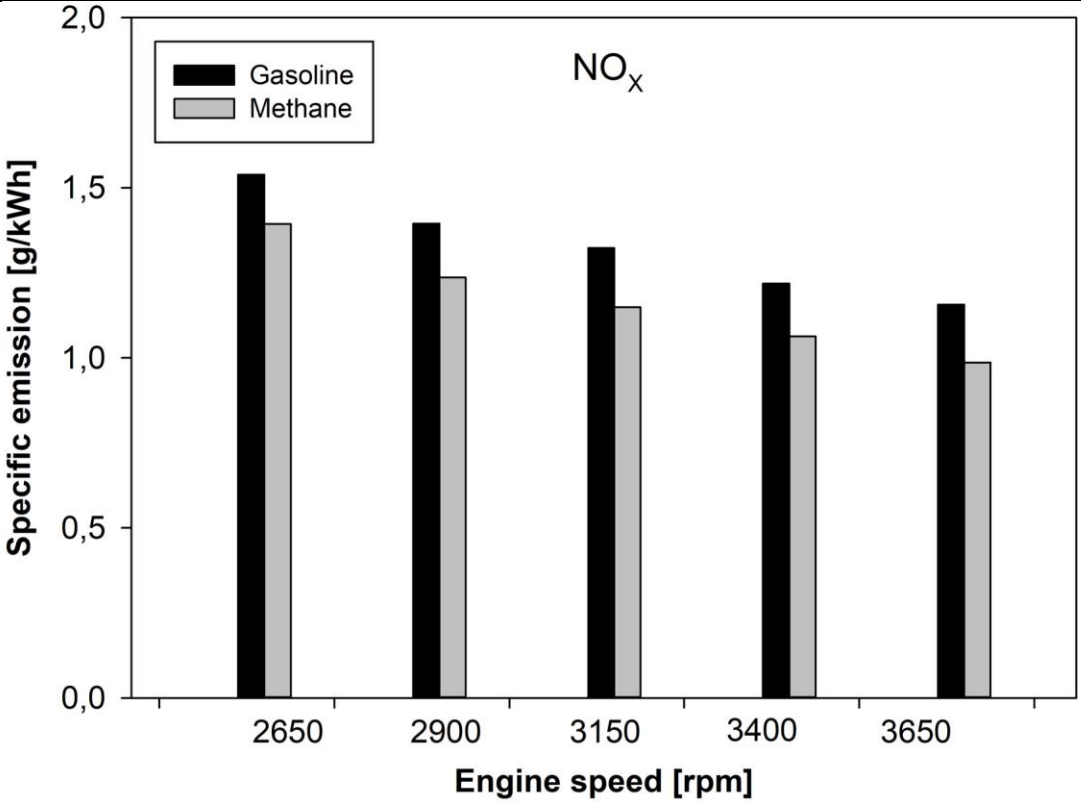

14-NOx